

Thermokinetic Analysis of the CO₂ Chemisorption on Li₄SiO₄ by Using Different Gas Flow Rates and Particle Sizes

Rafael Rodríguez-Mosqueda and Heriberto Pfeiffer*

Instituto de Investigaciones en Materiales, Universidad Nacional Autónoma de México, Circuito exterior s/n, Cd. Universitaria, Del. Coyoacán, CP 04510, México D.F., MEXICO

Received: December 3, 2009; Revised Manuscript Received: March 3, 2010

Lithium orthosilicate (Li₄SiO₄) was synthesized by solid-state reaction and then its CO₂ chemisorption capacity was evaluated as a function of the CO₂ flow rate and particle size. Initially, a Li₄SiO₄ sample, with a total surface area of 0.4 m²/g, was used to analyze the CO₂ chemisorption, varying the CO₂ flow between 30 and 200 mL/min. Results showed that CO₂ flows modify the kinetic regime from which CO₂ capture is controlled. In the first moments and at low CO₂ flows, the CO₂ capture is controlled by the CO₂ diffusion through the gas-film system, whereas at high CO₂ flows it is controlled by the CO₂ chemisorption reaction rate. Later, at larger times, once the carbonate–oxide external shell has been produced the whole process depends on the CO₂ chemisorption kinetically controlled by the lithium diffusion process, independently of the CO₂ flow. Additionally, thermokinetic analyses suggest that temperature induces a CO₂ particle surface saturation, due to an increment of CO₂ diffusion through the gas-film interface. To elucidate this hypothesis, the Li₄SiO₄ sample was pulverized to increase the surface area (1.5 m²/g). Results showed that increasing the surface particle area, the saturation was not reached. Finally, the enthalpy activation (ΔH^\ddagger) values were estimated for the two CO₂ chemisorption processes, the CO₂ direct chemisorption produced at the Li₄SiO₄ surface, and the CO₂ chemisorption kinetically controlled by the lithium diffusion, once the carbonate–oxide shell has been produced.

Introduction

Environmentally, CO₂ production, sequestration, storage, and/or reutilization are some of the most important issues to be solved in the near future, due to their direct impact with the greenhouse effect and Earth's temperature. In this sense, lithium ceramics have been studied as possible CO₂ captors, showing some interesting results.^{1–10} In fact, two of the most important properties of this kind of ceramics are: (1) The CO₂ chemisorption can be performed in a wide range of temperatures, from room temperature up to 650–710 °C,² and (2) Several of these materials are recyclable.^{2,4}

Among lithium ceramics, lithium orthosilicate (Li₄SiO₄) seems to be one of the most promising materials into this field. Li₄SiO₄ chemisorbs CO₂ according to the following reaction:^{2,7,10–19}



It has to be mentioned that previous works claimed that Li₂SiO₃ was not able to absorb CO₂.^{16,20} Then, more recent papers proposed that CO₂ absorption on Li₂SiO₃ does occur, but it is not kinetically favored, and it only occurs under very specific conditions.^{13,21}

Different kinds of approximations have been performed to analyze the CO₂ chemisorption process on lithium and in general alkaline ceramics. Some papers have reported variation as a function of the particle size,^{13,22,23} which is totally related to the surface area and its higher capacity to chemisorb

CO₂ obtaining better efficiencies. Other papers report that CO₂ chemisorption can be improved due to structural modifications on the ceramics (doping and solid-solutions synthesis)^{17,19,24–28} and some other papers have studied qualitatively the CO₂ concentration effect by mixing CO₂ with different gases such as N₂, Ar, or even dry air.^{3,7,15,29} In this last point, as it may be expected, it has been seen that by increasing the CO₂ concentration, capture increases as well, independently of the second gas. All these previous works have been done using different CO₂ flows, without paying much more attention to this variable. Only Lin and co-workers did a qualitative analysis of this factor, varying the CO₂ flow from 40 to 160 mL/min during the CO₂ capture on K-doped Li₂ZrO₃.²² From this analysis, authors suggested that with a CO₂ flow rate equal or higher than 160 mL/min “the CO₂ pressure increase is close to step function compared to the total uptake time”.²² In addition, it has to be remembered that CO₂ chemisorption on lithium ceramics corresponds to a reaction system where the gas contacts the solid, reacts with it, and then transforms it into a product that produces an external shell. Then, in order to continue the CO₂ chemisorption it is necessary that lithium atoms present into the ceramic bulk diffuse to the surface to react with CO₂. From the literature, it is well-known that for these systems some possible variables are the CO₂ diffusion through the gas-film and/or the lithium diffusion through the external product shell, which, in the first case, may be altered by varying the flow gas.³⁰ Therefore, the aim of this paper was to study the effect of the flow gas on the CO₂ chemisorption on Li₄SiO₄, one of the most promising lithium ceramics, and then to analyze kinetically the CO₂ chemisorption process at those different flow conditions.

* To whom correspondence should be addressed. Phone: +52 (55) 5622 4627. Fax: +52 (55) 5616 1371. E-mail: pfeiffer@iim.unam.mx.

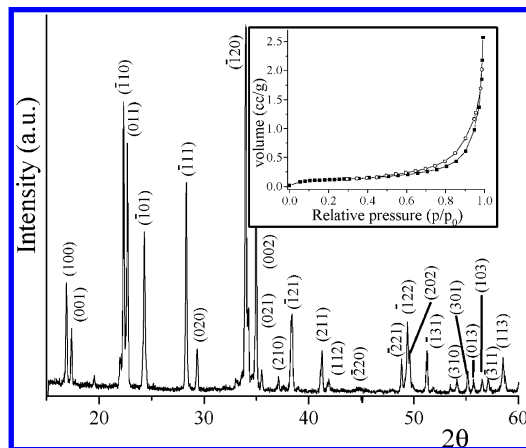


Figure 1. XRD pattern and N_2 adsorption–desorption isotherm (inset) of the Li_4SiO_4 sample.

Experimental Section

Li_4SiO_4 was synthesized by solid-state method, using lithium carbonate (Li_2CO_3 , Aldrich) and silica gel (SiO_2 , Merck). Initially, both powders were mechanically mixed. Then, the mixture was calcined at 850 °C for 8 h, with an intermediate mechanical milling. To improve the synthesis, 10 wt % of lithium excess was used, due to the high tendency of lithium to sublimate.

Sample was characterized by different techniques. For the X-ray diffraction (XRD) a diffractometer Bruker AXS D8 Advance was used coupled to a copper anode X-ray tube. Li_4SiO_4 was identified conventionally by its corresponding Joint Committee Powder Diffraction Standard (JCPDS) file. Nitrogen adsorption–desorption isotherms and BET surface area analyses were determined with a Bel-Japan Minisorp II equipment, at 77 K using a multipoint technique. Samples were previously degasified at 85 °C for 12 h in vacuum. Finally, different thermal analyses were performed in a Q500HR equipment from TA Instruments. Initially, a set of samples were heat-treated dynamically, with heating rates of 5 and 3 °C/min from room temperature to 700 °C into different CO_2 flows (from 30 to 200 mL/min). Then, Li_4SiO_4 sample was tested isothermally at different temperatures, into the same CO_2 flows.

Results and Discussion

Figure 1 presents the characterization of the Li_4SiO_4 sample prepared by solid-state method. The XRD pattern fitted to the 37–1472 JCPDS file, which implies that only the Li_4SiO_4 phase is present in the powder. Additionally, a textural analysis was performed, where the Li_4SiO_4 sample presented an adsorption/desorption isotherm of type II (inset of Figure 1), exhibiting a very narrow H3 type hysteresis loop, according to the IUPAC classification.³¹ This behavior corresponds to nonporous materials. Then, the surface area was determined using the BET method, obtaining a surface area of 0.4 m²/g, which is in total agreement with the method of synthesis utilized; solid-state reaction.

Once the Li_4SiO_4 sample was characterized, the material was thermally treated under different CO_2 flows into a thermobalance, heating samples at 5 °C/min (Figure 2). Initially, all the thermograms seem to present similar behaviors. At temperatures lower than 300 °C all the thermograms are very stable. Then, between 300 and 400 °C the samples lost around 1 wt %, which may be attributed to superficial dehydroxylation. It has been already reported that Li_4SiO_4 is able to react with water steam

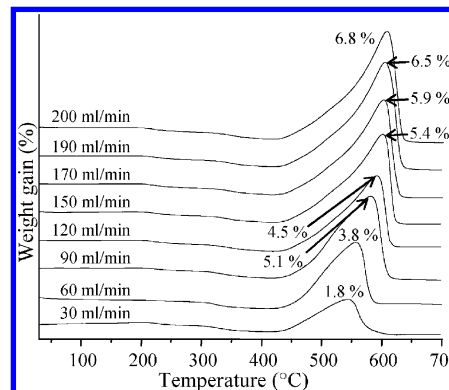


Figure 2. Dynamic thermograms of the Li_4SiO_4 , using a heating rate of 5 °C/min and different CO_2 flows. Numbers in each thermogram correspond to the maxima weight gain.

at room temperature.² Then, as this sample was exposed to the environment, some hydroxylation must have occurred. Finally, between 400 and 650 °C the main processes occurred. Initially all the samples presented an increment of weight, associated to the carbonation process. Several aspects must be pointed out from this part of the thermograms. Although the chemisorption process practically began at the same temperature (425 °C) for all the samples, the maxima CO_2 chemisorption temperature was not the same. Sample treated with a CO_2 flow of 30 mL/min presented the maxima chemisorption at 543.7 °C. Then, samples heat treated with 60, 90, 120, 150, 170, and 190 mL/min CO_2 flows shifted temperature to 556.8, 581.7, 592.6, 596.9, 602.7, and 603.5 °C, respectively. This temperature trend finalized up to 609.5 °C, which was the maxima CO_2 chemisorption temperature for the sample treated into a CO_2 flow of 200 mL/min. Thus, varying the CO_2 flow from 30 to 200 mL/min, chemisorption temperature was increased in 65.8 °C. To explain this thermal behavior it should be considered that those maxima temperatures correspond, equally, to the initial desorption temperature. Therefore, if the CO_2 flows modify the CO_2 diffusion through the gas-film, according to theoretical analyses,³⁰ the equilibrium may be shifted to the right due to a higher presence of CO_2 molecules into the gas-film (near to the surface particles), as a function of the CO_2 flow. Additionally, in a previous study it was shown, isothermally for other lithium ceramic (lithium metazirconate, Li_2ZrO_3), that at CO_2 flows of 160 mL/min or higher the CO_2 pressure is close to step function compare to the total uptake time.²² This reference and the present work seem to be in good agreement, as the maxima shift on the chemisorption temperature, observed in this work, was around 150–170 mL/min. At higher CO_2 flows the maxima chemisorption temperature varied more slowly. All these results suggest that varying the CO_2 flow may modify the kinetic regime from which CO_2 chemisorption is controlled. Although in CO_2 flows lower than 150 mL/min the gas-film, over the particle surface,³⁰ controls the process; in CO_2 flows equal to or higher than 150 mL/min the process is controlled by the CO_2 chemisorption reaction rate. This is only valid in the first moments of the whole process, before the lithium carbonate external shell is produced.

From these thermograms two other differences became evident. First, although it is a qualitative analysis, the CO_2 chemisorbed seems to be increased as a function of the CO_2 flow. In fact, while the sample treated with a CO_2 flow of 30 mL/min only increased its weight by 1.8 wt %, the sample treated with a CO_2 flow of 200 mL/min gained up to 6.8 wt %, which is almost four times more CO_2 . Additionally, the CO_2

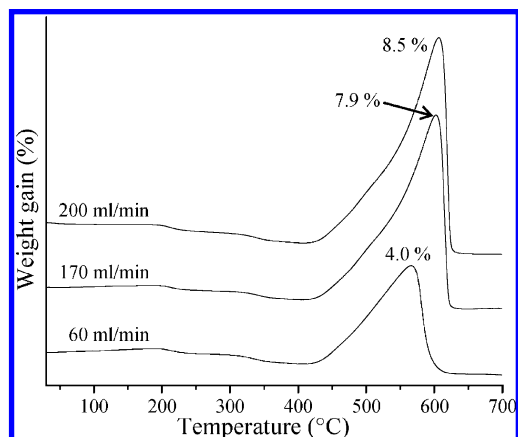


Figure 3. Dynamic thermograms of the Li₄SiO₄, using a heating rate of 3 °C/min and different CO₂ flows. Numbers in each thermogram correspond to the maxima weight gain.

chemisorption slopes observed on the different samples changed as a function of the CO₂ flow, meaning that kinetic factors are modified as a function of the CO₂ flow. All these results strongly suggest that CO₂ chemisorption on Li₄SiO₄ does not only depend on temperature, but on CO₂ flow as well.

To further elucidate the kinetic dependency of the CO₂ chemisorption on Li₄SiO₄, a sample was analyzed dynamically again but using a different heating rate (3 °C/min) with the following CO₂ flows: 60, 170, and 200 mL/min (Figure 3). In these cases, the general behavior was the same. The initial temperature for the CO₂ chemisorption process occurred at 423 °C, which is practically the same temperature observed in the previous case (425 °C). However, the maxima CO₂ chemisorption temperatures tended to be shifted to higher temperatures, 565.6, 602.7, and 607 °C for the CO₂ flows of 60, 170, and 200 mL/min, respectively. Finally, the total CO₂ chemisorbed increased, again, as a function of the CO₂ flow, from 4.0 to 8.5 wt %.

As the dynamic thermogravimetric studies involved kinetic implications on the CO₂ chemisorption on Li₄SiO₄, using different CO₂ flows, a kinetic analysis was performed with isothermal experiments. Figure 4 shows the different isotherms performed varying temperature and CO₂ flow. Initially, isotherms at different temperatures using a CO₂ flow of 60 mL/min are shown in Figure 4A. At the lowest temperature (460 °C), the isothermal showed an exponential behavior, trapping 5.2 wt % of CO₂ after 3 h, and it did not reach a plateau. Then, samples treated between 480 and 540 °C presented the same exponential behavior, increasing their weights up to 11.3 wt %. However, the sample treated at 560 °C presented an atypical behavior. This isotherm trapped less CO₂, 10.8 wt %, in comparison to the sample treated at 540 °C. In this specific case, it should be taken into account that this isotherm was performed over the chemisorption–desorption temperature limit, as the maxima CO₂ chemisorption temperature in the dynamic process was 556.8 °C (see Figure 2). Then, at these specific conditions, Li₄SiO₄ is chemisorbing CO₂, but at the same time, the Li₂CO₃ produced must decompose and desorb CO₂. In fact, the desorption process must be slower than the chemisorption process, and as the isotherm did not reach the plateau, chemisorption–desorption equilibrium has not been reached.

Figures 4B and 4C show the isotherms performed at CO₂ flows of 150 and 170 mL/min. In both cases, the same exponential behavior was obtained. At a CO₂ flow of 150 mL/min, CO₂ chemisorption increased as a function of temperature from 7.7 to 16.3 wt % for 460 and 560 °C, respectively. In this

flow conditions (150 mL/min), the CO₂ chemisorption was higher in all the temperature range and the isotherm performed at 560 °C did not behave atypically. Of course, this isotherm did not present the desorption process, as the maxima CO₂ chemisorption temperature was shifted up to 596.9 °C (see figure 2). As mentioned previously, isotherms performed with a 170 mL/min flow behave as the 150 mL/min case. There was no significant variation among them.

Figure 4D presents the isotherms performed with a CO₂ flow of 200 mL/min. In this case, a different behavior was observed. While the sample heat treated at 460 °C captured 6.8 wt %, samples heat treated at 480 and 500 °C trapped only 5.8 and 6.2 wt %, respectively. Nevertheless, these two samples showed a faster CO₂ chemisorption, at short times, than that observed at 460 °C (see inset of Figure 4D). This behavior has already been reported for the CO₂ chemisorption on other alkaline ceramics such as Na₂ZrO₃, Li₅AlO₄, and Li₂CuO₂.^{9,32,33} This effect has been associated with a sintering process of the sample, which produces an important decrement of the surface area, thereby inhibiting the reaction. This phenomenon is usually observed only at lower temperatures because once the lithium diffusion process is activated, sintering and surface area are not preponderant factors, any more, on the CO₂ chemisorption process. In this case, as the CO₂ flow is considerably high (200 mL/min), the sintered Li₄SiO₄ surface may be saturated with CO₂ and the whole process should only depend on the reaction rate. Additionally, it has to be taken into account that the initial surface area of this sample is very small, 0.4 m²/g.

Most of the isotherms were fitted to a double exponential model (eq 2,¹⁹), assuming that there are only two different processes taking place during the CO₂ capture on Li₄SiO₄: (1) CO₂ chemisorption, initially, is produced directly by the reaction between the CO₂ molecules and the Li₄SiO₄ surface (k_1); and (2) Once the carbonate-oxide external shell is totally formed, CO₂ chemisorption is kinetically controlled by lithium diffusion (k_2). The double exponential model to which the isotherms were fitted is:

$$y = A \exp^{-k_1 t} + B \exp^{-k_2 t} + C \quad (2)$$

where, y represents the weight percentage of CO₂ chemisorbed; t is the time; and k_1 and k_2 are the exponential constants for the CO₂ chemisorption produced directly over the Li₄SiO₄ particles and CO₂ chemisorption kinetically controlled by lithium diffusion, respectively. Additionally, the pre-exponential factors A and B indicate the intervals at which each process controls the whole CO₂ capture process, and the C constant indicates the y -intercept. It has to be added that this model was used establishing the following assumptions. None of the samples reached or enhanced the maxima CO₂ absorption capacity (36.66 wt %, according to reaction 1), which could imply that Li₂SiO₃ absorbed CO₂ as well. Additionally, it is well-known that the kinetic behavior of CO₂ absorption on Li₂SiO₃ is much slower than that on Li₄SiO₄.^{13,21}

Table 1 shows the CO₂ direct chemisorption (k_1) and chemisorption kinetically controlled by lithium diffusion (k_2) constant values obtained for the different CO₂ flows, including the pre-exponential constants and R² values. Initially, it can be seen that k_1 values are, in general, 1 order of magnitude higher than those obtained for the k_2 constants, independently of the CO₂ flow. Additionally, B constants are always larger than A constants values. It means that CO₂ chemisorption, kinetically controlled by lithium diffusion, occurs in a larger interval of time than CO₂ chemisorption produced directly over the particle

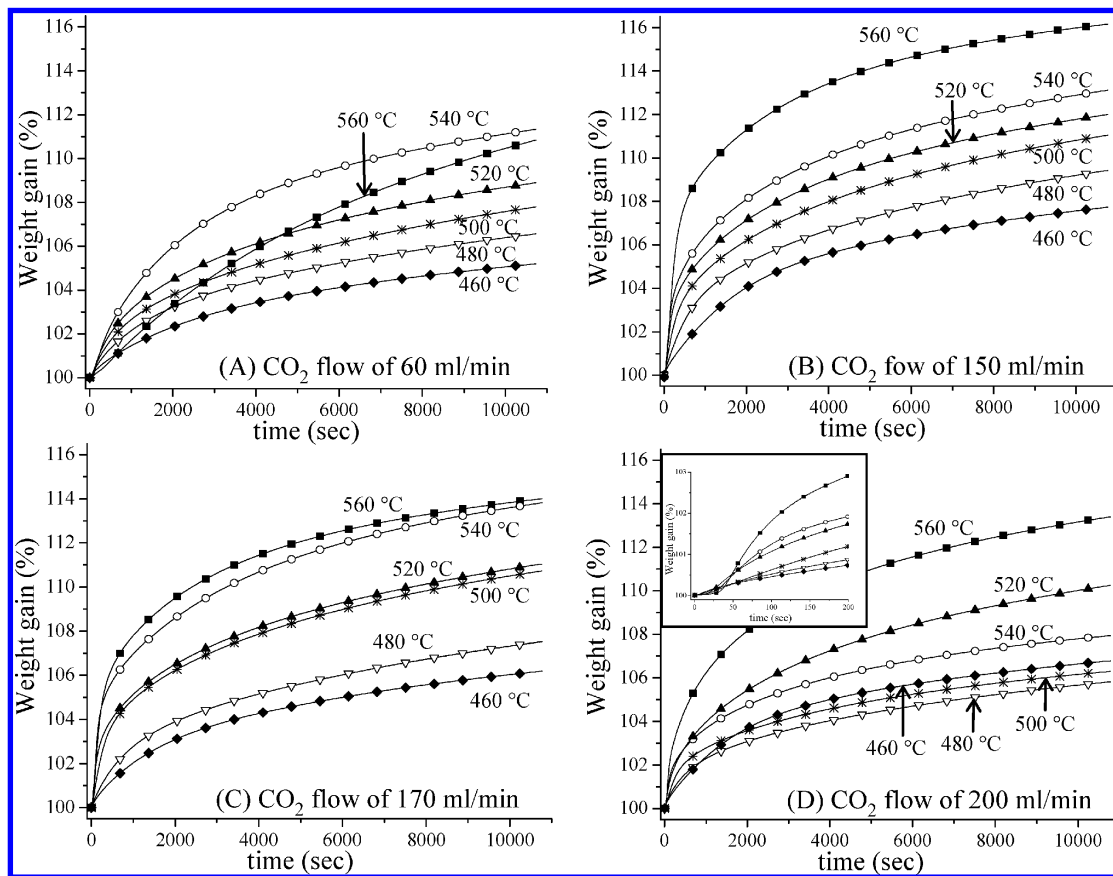


Figure 4. Isotherms of CO₂ chemisorption on Li₄SiO₄ at 460, 480, 500, 520, 540, and 560 °C, using different CO₂ flows.

surfaces. These results are in total agreement with the fact that CO₂ direct chemisorption occurs initially over the particle surface, but the main content of material is into the bulk of the ceramic and it is necessary for the lithium diffusion to produce it. All these results show that CO₂ chemisorption kinetically controlled by lithium diffusion is the limiting step of the whole CO₂ capture process. These results are in agreement to previous results published about the CO₂ chemisorption on Li₄SiO₄ and other lithium ceramics.^{9,19,33}

To analyze quantitatively the temperature and CO₂ flow dependence of the two different processes, the Eyring's model was used (eq 3), as it can be used on solid–gas systems:

$$\ln(k_i/T) = -(\Delta H_i^\ddagger/R)(1/T) + \ln E + \Delta S_i^\ddagger/R \quad (3)$$

where, k_i is the rate constant value of the process i ; E represents a pre-exponential factor, which in Eyring's formulation is equal to the ratio of Boltzmann's constant to Planck's constant; R is the ideal gas constant and ΔH_i^\ddagger and ΔS_i^\ddagger are the activation enthalpy and entropy, respectively.

From Figure 5, it is clear that only the plots of CO₂ chemisorption kinetically controlled by lithium diffusion describe totally linear trends (Figure 5B), fitting Eyring's model, where the average ΔH_i^\ddagger was equal to 37.2 ± 10 kJ/mol. On the contrary, k_1 plots only describe partial linear trends at low temperatures (Figure 5A), showing a more complex behavior. In this case, the ΔH_i^\ddagger values increased as a function of the CO₂ flow as follows: 94.4, 128.4, 124.4, and 157.8 kJ/mol, fitting the CO₂ flow at 60, 150, 170, and 200 mL/min, respectively. These results indicate that CO₂ direct chemisorption reaction is more dependent on temperature than CO₂ chemisorption kinetically controlled by lithium diffusion.

All these kinetic results show that although the CO₂ chemisorption kinetically controlled by lithium diffusion does not seem to change, by varying the CO₂ flow the CO₂ direct chemisorption did change. However, according to the different k values, it was established as well that CO₂ capture is kinetically controlled by lithium diffusion. Therefore, the CO₂ flow must only affect the whole process on the first moments, when there is a reaction, but there is not lithium diffusion. Additionally, Eyring's plots show that there are two different phenomena controlling the CO₂ direct chemisorption reaction, which vary as a function of temperature. At low temperatures, where a linear trend was observed, the reaction should be controlled by the gas-film system.³⁰ In this case, CO₂ direct chemisorption depends on the CO₂ quantities approaching the particle surface, assuming that CO₂ diffusion through the gas-film is slower than the CO₂ chemisorption reaction. Then, high temperatures should produce a particle surface saturation, due to an increment of CO₂ diffusion through the gas-film interface. Thus, under these new conditions, CO₂ chemisorption only depends on the reaction rate, during the first instants. At larger times CO₂ capture is always kinetically controlled by lithium diffusion.

To corroborate the particle surface saturation, the same Li₄SiO₄ sample was pulverized in order to increase its surface area. The new surface area obtained was equal to 1.5 m²/g, which is almost four times larger than that obtained for the original sample. Figure 6 shows the dynamic and isothermal experiments performed for the CO₂ chemisorption with the pulverized sample. The dynamic thermogram (Figure 6A) shows a similar behavior to the original sample, as it could be expected. Initially, the sample was stable up to 230 °C. Then, between 230 and 420 °C the sample lost around 1.3 wt %, attributed to superficial dehydroxylation. Later, the CO₂ chemisorption

TABLE 1: Li₄SiO₄ Kinetic Parameters Obtained by Using Different CO₂ Flows

<i>T</i> (°C)	<i>k</i> ₁ (sec ⁻¹)	<i>k</i> ₂ (sec ⁻¹)	<i>A</i>	<i>B</i>	<i>C</i> ^a	<i>R</i> ²
CO ₂ Flow of 60 mL/min ^b						
460	7.9 × 10 ⁻⁴	1.2 × 10 ⁻⁴	-1.466	-4.934	106.4	0.9991
480	1.02 × 10 ⁻³	1.0 × 10 ⁻⁴	-2.345	-6.414	108.8	0.9994
500	1.56 × 10 ⁻³	1.2 × 10 ⁻⁴	-2.357	-7.689	110.0	0.9994
520	1.66 × 10 ⁻³	1.5 × 10 ⁻⁴	-2.680	-7.927	110.5	0.9998
540	1.05 × 10 ⁻⁴	1.8 × 10 ⁻⁴	-4.067	-8.616	112.5	0.9998
CO ₂ Flow of 150 mL/min						
460	8.0 × 10 ⁻⁴	1.4 × 10 ⁻⁴	-3.248	-5.560	108.8	0.9997
480	1.72 × 10 ⁻³	1.3 × 10 ⁻⁴	-3.467	-7.821	111.2	0.9994
500	2.96 × 10 ⁻³	1.7 × 10 ⁻⁴	-3.716	-8.668	112.3	0.9996
520	4.26 × 10 ⁻³	2.1 × 10 ⁻⁴	-4.231	-8.711	112.8	0.9991
540	4.17 × 10 ⁻³	2.1 × 10 ⁻⁴	-4.983	-9.003	113.8	0.9987
560	4.27 × 10 ⁻³	2.5 × 10 ⁻⁴	-9.017	-8.911	116.6	0.9992
CO ₂ Flow of 170 mL/min						
460	8.5 × 10 ⁻⁴	9.0 × 10 ⁻⁵	-2.443	-5.696	108.2	0.9999
480	1.38 × 10 ⁻³	1.0 × 10 ⁻⁴	-2.673	-7.090	109.8	0.9996
500	3.05 × 10 ⁻³	1.6 × 10 ⁻⁴	-4.072	-8.090	112.0	0.9996
520	3.96 × 10 ⁻³	1.8 × 10 ⁻⁴	-3.664	-8.130	112.0	0.9989
540	6.25 × 10 ⁻³	2.2 × 10 ⁻⁴	-5.848	-9.398	114.5	0.9991
560	4.67 × 10 ⁻³	2.6 × 10 ⁻⁴	-6.917	-8.295	114.3	0.9989
CO ₂ Flow of 200 mL/min						
460	7.4 × 10 ⁻⁴	1.0 × 10 ⁻⁴	-3.512	-4.826	108.4	0.9999
480	1.83 × 10 ⁻³	1.2 × 10 ⁻⁴	-1.862	-5.124	107.1	0.9998
500	2.97 × 10 ⁻³	1.6 × 10 ⁻⁴	-2.205	-4.881	107.0	0.9996
520	2.11 × 10 ⁻³	1.7 × 10 ⁻⁴	-2.672	-8.547	111.5	0.9995
540	3.38 × 10 ⁻³	2.1 × 10 ⁻⁴	-2.537	-5.698	108.4	0.9988
560	2.39 × 10 ⁻³	2.1 × 10 ⁻⁴	-4.603	-9.232	114.2	0.9990

^a Values varied from 100 as a consequence of the initial dead times and variation of mass (dehydration) presented in each isothermal experiment. ^b The isothermal experiment performed at 560 °C, with this CO₂ flow, was not fitted to the double exponential model as it was presented for the CO₂ desorption.

process began at 435 °C. It means that the CO₂ chemisorption initial temperature was shifted 10 °C to higher temperatures, in comparison to the original sample. A similar effect was observed on the maxima CO₂ chemisorption temperature, which in this case was shifted from 556.8 °C up to 608.2 °C. All these changes on the thermal behavior should be attributed to a higher surface area, which promotes a higher CO₂ chemisorption. This assumption was confirmed qualitatively by the total weight gained in this dynamic process, which increased from 4.5 to 6.6 wt %, for the original and the pulverized samples, respectively.

Isothermal curves of the pulverized sample presented a similar behavior to that observed for the original one, using a CO₂ flow of 60 mL/min. At 460 °C, the isothermal showed an exponential behavior, trapping 5.7 wt % of CO₂ after 3 h. Then, samples treated between 480 and 540 °C presented the same exponential behavior, increasing their weights from 7.6 to 12.5 wt %. In this case, this sample always captured more CO₂ than the original sample, again due to the surface area. Additionally, sample treated at 560 °C did not present the atypical behavior observed on the original sample, as the maxima CO₂ chemisorption temperature was shifted to higher temperatures.

Again, these isotherms were fitted to a double exponential model, and then the *k* values were fitted to the Eyring's model. The kinetic parameters obtained in this case are presented in the Table 2. If these values are compared with the corresponding data of the sample before being pulverized (Table 1), it can be seen that none of the constant values (*k*₁ or *k*₂) varied significantly. In fact, only the parameter *A* showed a significant difference, being in this case larger. This result indicates that

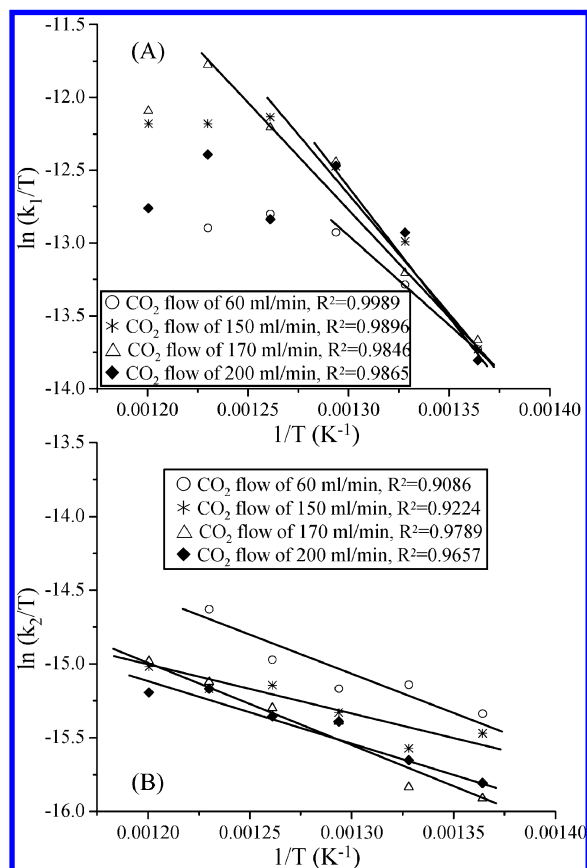


Figure 5. Eyring's plots of the two different CO₂ chemisorption processes: (A) direct chemisorption and (B) chemisorption kinetically controlled by lithium diffusion, using different CO₂ flows.

CO₂ direct chemisorption (*k*₁) occurs in a larger interval of time than, which is in total agreement with a larger surface area. Moreover, Figure 7 compares the ln(*k*₁/T) vs 1/*T* plots of the CO₂ direct chemisorption process of both Li₄SiO₄ samples, with different surface areas, as well as a different sample reported previously.¹⁹ As it can be seen, Li₄SiO₄ pulverized sample did described a linear trend in the whole temperature range, in comparison to the initial sample, which only described this trend at low temperatures. It seems that if the surface area is increased, the CO₂ does not saturate the Li₄SiO₄ particle surface, and thus the reaction is controlled by the gas-film system in the whole range of temperatures. Δ*H*[‡] value, for the CO₂ direct chemisorption process, was equal to 83.4 kJ/mol, which is close to the 94.4 kJ/mol value obtained initially. These energy values are, in fact, very similar to the previously reported Δ*H*[‡] value of 88.9 kJ/mol, which corresponds to a Li₄SiO₄ sample with a larger surface area, 3 m²/g.¹⁹ Finally, Δ*H*[‡] of the CO₂ chemisorption kinetically controlled by lithium diffusion was determined for the Li₄SiO₄ pulverized, and it was equal to 32 kJ/mol. This result is in good agreement with the previous values obtained initially, 37.2 ± 10 kJ/mol on average.

Conclusions

Once Li₄SiO₄ was synthesized by solid-state reaction (surface area 0.4 m²/g), it was tested as CO₂ captor, using different CO₂ flows (30–200 mL/min). The initial dynamic results suggested that CO₂ chemisorption on Li₄SiO₄ depends not only on temperature, but also on the CO₂ flow. On the basis of the dynamic results, a kinetic analysis was performed as well, which confirmed the CO₂ capture dependency on the CO₂ flow. In fact,

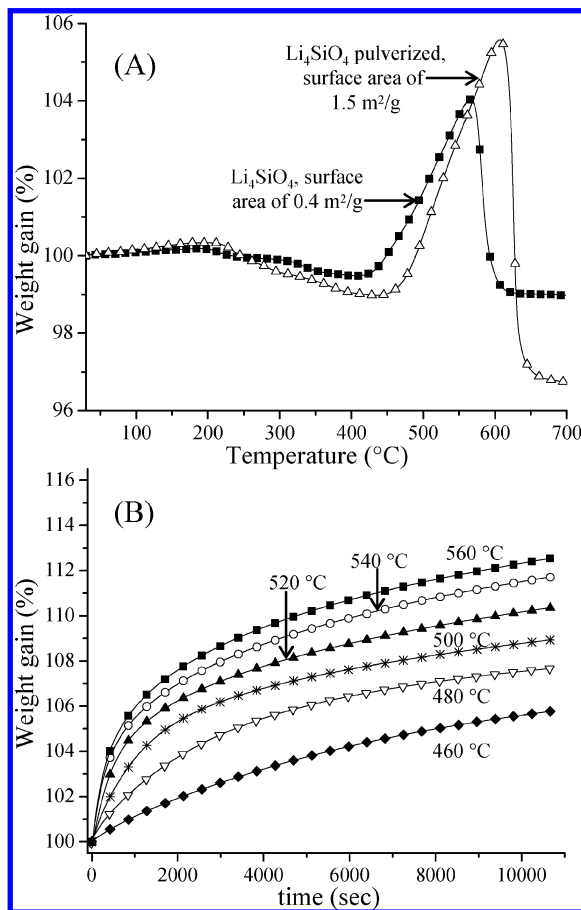


Figure 6. Dynamic (A) and isothermal (B) thermogravimetric curves for the Li_4SiO_4 pulverized. In the dynamic graph (A) the initial thermogram is presented again for comparison reasons. All these experiments were performed using a CO_2 flow of 60 mL/min.

TABLE 2: Kinetic Parameters Obtained for the Li_4SiO_4 Sample with a Surface Area Equal to 1.5 m^2/g , Using a CO_2 Flow of 60 mL/min

T ($^\circ\text{C}$)	k_1 (sec^{-1})	k_2 (sec^{-1})	A	B	C^a	R^2
460	5.8×10^{-4}	1.2×10^{-4}	-0.349	-7.363	107.803	0.9999
480	7.5×10^{-4}	1.9×10^{-4}	-2.051	-6.274	108.472	0.9998
500	1.04×10^{-3}	1.1×10^{-4}	-4.693	-6.191	110.899	0.9999
520	1.9×10^{-3}	1.4×10^{-4}	-4.647	-7.409	111.882	0.9998
540	2.5×10^{-3}	1.6×10^{-4}	-4.632	-8.517	113.175	0.9996
560	2.94×10^{-3}	1.7×10^{-4}	-4.976	-8.788	113.853	0.9996

^a Values varied from 100 as a consequence of the initial dead times and variation of mass (dehydration) presented in each isothermal experiment.

results showed that CO_2 flows modify the kinetic regime from which CO_2 capture is controlled, as follows: In the first moments, at low CO_2 flows (<150 mL/min), the process is controlled by a gas-film system. On the contrary, at high CO_2 flows (≥ 150 mL/min) the CO_2 chemisorption is controlled by the CO_2 chemisorption reaction rate, as the solid-gas interface must be totally saturated of CO_2 . Later, once the Li_2CO_3 - Li_2SiO_3 external shell is formed, the whole process depends on the bulk lithium diffusion process, independently of the CO_2 flow.

Kinetic constants showed that lithium diffusion is the limiting process on the whole CO_2 capture process, independently of the CO_2 flow. Additionally, fitting these data to the Eyring's model showed that the average activation enthalpy (ΔH^\ddagger) for the CO_2 chemisorption controlled by the lithium diffusion

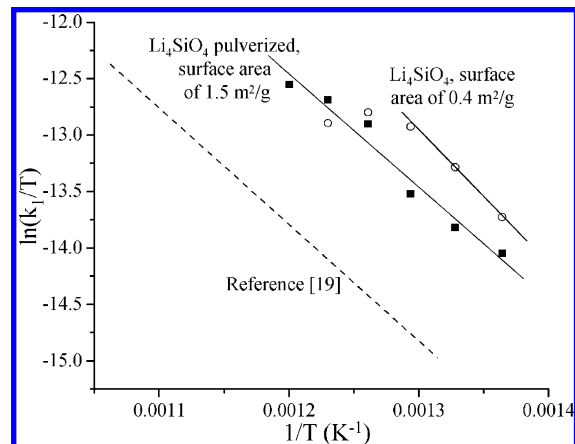


Figure 7. Eyring's plots of the CO_2 direct chemisorption process on Li_4SiO_4 for different samples, using the similar CO_2 flows.

process was equal to 37.2 ± 10 kJ/mol, independently of the CO_2 flow. On the contrary, CO_2 direct chemisorption (sample with 0.4 m^2/g of surface area) plots only describe partial linear trends at low temperatures. The ΔH^\ddagger values increased as a function of the CO_2 flow from 94.4 to 157.8 kJ/mol, varying CO_2 flows from 60 to 200 mL/min, respectively. It seems that CO_2 direct chemisorption reaction is more dependent on temperature than the CO_2 chemisorption kinetically controlled by the lithium diffusion process and higher CO_2 flows implies a higher dependence of the CO_2 direct chemisorption process as well. The partial linear fit of these data was interpreted in terms a CO_2 surface saturation, due to an increment of CO_2 diffusion through the gas-film interface. To corroborate this hypothesis, a Li_4SiO_4 sample was pulverized (new surface area 1.5 m^2/g). Results showed that if the surface area is increased, there is no surface particle saturation at the corresponding flows and, at the first moments, CO_2 chemisorption is controlled by the gas-film system in the whole temperature range. On the Li_4SiO_4 sample, with a larger surface area (1.5 m^2/g), ΔH^\ddagger value for the direct CO_2 chemisorption was 83.4 kJ/mol and for the CO_2 chemisorption kinetically controlled by lithium diffusion was 32 kJ/mol. These values are very similar to those obtained for the same sample with a smaller surface area.

Acknowledgment. This work was performed into the IMPULSA-PUNTA framework of the Universidad Nacional Autónoma de México and financially supported by CONACYT-SEMARNAT (23418), ICyT-DF (179/2009), and PAPIIT-UNAM (IN100609). The authors thank L. Baños, A. Tejada, and E. Fregoso for technical help.

References and Notes

- (1) Nakagawa, K.; Ohashi, T. *J. Electrochem. Soc.* **1998**, *145*, 1344–1347.
- (2) Nair, B. N.; Burwood, R. P.; Goh, V. J.; Nakagawa, K.; Yamaguchi, T. *Prog. Mater. Sci.* **2009**, *54*, 511–541.
- (3) Ochoa-Fernández, E.; Rønning, M.; Yu, X.; Grande, T.; Chen, D. *Ind. Eng. Chem. Res.* **2008**, *47*, 434–442.
- (4) Yi, K. B.; Eriksen, D. Ø. *Sep. Sci. Technol.* **2006**, *41*, 283–296.
- (5) Pfeiffer, H.; Bosch, P. *Chem. Mater.* **2005**, *17*, 1704–1710.
- (6) Togashi, N.; Okumura, T.; Oh-ishi, K. *J. Ceram. Soc. Japan* **2007**, *115*, 324–328.
- (7) Kato, M.; Nakagawa, K.; Essaki, K.; Maezawa, Y.; Takeda, S.; Kogo, R.; Hagiwara, Y. *Inter. J. Appl. Ceram. Tech.* **2005**, *2*, 467–475.
- (8) Palacios-Romero, L. M.; Pfeiffer, H. *Chem. Lett.* **2008**, *37*, 862–863.
- (9) Ávalos-Rendón, T. L.; Casa-Madrid, J. A.; Pfeiffer, H. *J. Phys. Chem. A* **2009**, *113*, 6919–6923.
- (10) Essaki, K.; Kato, M.; Uemoto, H. *J. Mater. Sci.* **2005**, *18*, 5017–5019.

- (11) Okumura, T.; Enomoto, K.; Togashi, N.; Oh-ishi, K. *J. Ceram. Soc. Japan* **2007**, *115*, 491–497.
- (12) Essaki, K.; Nakagawa, K.; Kato, M.; Uemoto, H. *J. Chem. Eng. Jpn.* **2004**, *37*, 772–777.
- (13) Khomane, R. B.; Sharma, B.; Saha, S.; Kulkarni, B. D. *Chem. Eng. Sci.* **2006**, *61*, 3415–3418.
- (14) Kato, M.; Maezawa, Y.; Takeda, S.; Hagiwara, Y.; Kogo, R.; Semba, K.; Hamamura, M. *Key Eng. Mater.* **2006**, *317–318*, 81–84.
- (15) Kato, M.; Yoshikawa, S.; Nakagawa, K. *J. Mater. Sci. Lett.* **2002**, *21*, 485–487.
- (16) Tsumura, N.; Kuramoto, A.; Shimamoto, Y.; Aono, H.; Sadaoka, Y. *J. Ceram. Soc. Japan* **2005**, *113*, 269–274.
- (17) Gauer, C.; Heschel, W. *J. Mater. Sci.* **2006**, *41*, 2405–2409.
- (18) Yamaguchi, T.; Niitsuma, T.; Nair, B. N.; Nakagawa, K. *J. Membr. Sci.* **2007**, *294*, 16–21.
- (19) Mejia-Trejo, V. L.; Fregoso-Israel, E.; Pfeiffer, H. *Chem. Mater.* **2008**, *20*, 7171–7176.
- (20) Kato, M.; Nakagawa, K. *J. Ceram. Soc. Japan* **2001**, *109*, 911–914.
- (21) Venegas, M. J.; Fregoso-Israel, E.; Escamilla, R.; Pfeiffer, H. *Ind. Eng. Chem. Res.* **2007**, *46*, 2407–2412.
- (22) Xiong, R.; Ida, J.; Lin, Y. S. *Chem. Eng. Sci.* **2003**, *58*, 4377–4385.
- (23) Choi, K. H.; Korai, Y.; Mochida, I. *Chem. Lett.* **2003**, *32*, 924–925.
- (24) Ida, J.; Xiong, R.; Lin, Y. S. *Separ. Purif. Tech.* **2004**, *36*, 41–51.
- (25) Pannocchia, G.; Puccini, M.; Seggiani, M.; Vitolo, S. *Ind. Eng. Chem. Res.* **2007**, *46*, 6696–6706.
- (26) Veliz-Enriquez, M. Y.; Gonzalez, G.; Pfeiffer, H. *J. Solid State Chem.* **2007**, *180*, 2485–2492.
- (27) Pfeiffer, H.; Lima, E.; Bosch, P. *Chem. Mater.* **2006**, *18*, 2642–2647.
- (28) Pfeiffer, H.; Sánchez-Sánchez, J.; Álvarez, L. J. *J. Nucl. Mater.* **2000**, *280*, 295–303.
- (29) Zhao, T.; Ochoa-Fernández, E.; Rønning, M.; Chen, D. *Chem. Mater.* **2007**, *19*, 3294–3301.
- (30) Levenspiel, O. *Chemical Reaction Engineering*, 3rd ed.; John Wiley & Sons: USA, 1999; pp 566–588.
- (31) Lowell, S.; Shields, J. E.; Thomas, M. A.; Thommes, M. *Characterization of Porous Solids and Powders: Surface Area, Pore Size and Density*; Kluwer Acad. Press: Dordrecht, The Netherlands, 2004.
- (32) Palacios-Romero, L. M.; Lima, E.; Pfeifer, H. *J. Phys. Chem. A* **2009**, *113*, 193–198.
- (33) Alcérreca-Corte, I.; Fregoso-Israel, E.; Pfeiffer, H. *J. Phys. Chem. C* **2008**, *112*, 6520–6525.

JP911491T